Pergamon

Int. J. Heat Mass Transfer. Vol. 40, No. 17, pp. 4197–4208, 1997

Printed in Great Britain
0017–9310/97 $17.00+0.00

PII: S0017–9310(97)00025–2

Enhancement of mass transfer coefficients in spiral films

L. BRONIARZ-PRESS

Department of Chemical Engineering and Apparature, Poznań University of Technology, PL 60-965 Poznań, pl. M. Sklodowskiej-Curie 2, Poznań, Poland

(*Received* 9 *August* 1995 *and in final form* 22 *November* 1996)

Abstract—The wetted columns both with tangential nozzles and turbulence promoters are of great interest. The spiral motion of a liquid film gives a good stability and a great turbulence to the film. It results in the increase of the rate of transfer processes compared with those both in smooth and rough wall columns. The liquid phase mass transfer coefficients for the absorption of carbon dioxide into water have been measured on three types of threaded surfaces. The enhancement film mass transfer criteria have been proposed. The positive effect of surface ribbing in a helix in comparison with similar form incisions perpendicular to apparatus axis has been shown. © 1997 Elsevier Science Ltd.

INTRODUCTION

The imposition of the spiral motion on a liquid layer increases both the uniformity of the surface wettability and the stability of the film flow. It significantly affects both the inlet section length and the increase of turbulence of thin layer in comparison with these ones in a falling film apparatus. The following two methods can be used to induce the passive swirlization of a liquid film: application of the wetting device with tangential nozzles or incisions along the helix and imposing of regular wall roughness in a form of incisions or wiring in a helix on the total active height of an apparatus. In the first case it is more reasonable to use the qualitification of "pre-swirlization", since the "spiral film" in Carre and Bugarel formulation [1] exists only in the upper part of a column on so-called "effective" length. Below this length the film flows gravitationally. In experimental studies [1] the hydrodynamical characteristics, interface phenomena as well as the rate and the efficiency of carbon dioxide absorption from air into water and sodium hydroxide solution at $Re_e \in (106; 10\,600)$ have been investigated. For low inlet velocities of liquid the falling film without smooth entrance length has existed practically on the whole active height of apparatus. For inlet velocities of the magnitude of 10 m s^{-1} the waves have been decayed. The higher turbulization of film flow induced the more complex interference phenomena than these observed in falling film. The mean film thickness was lower than in falling film. The rise of turbulent mechanism was observed at lower Reynolds numbers. The efficiency of the column with tangential nozzles increased four times in relation to falling film apparatus and the minimal wetting rate decreased from four to five times. The maximal increase in the value of liquid phase mass transfer coefficient was 3.5 times. The measurements reported in [2] showed that the appearance of the unitary interface surface depends on: the distance from liquid inlet, the velocity of liquid in a mass nozzle, the Reynolds number in gas phase and the surface wetting rate. The gas phase mass transfer coefficient, dependent on the increase of interface area and the effective height of a column, was on the average from 2 to 3 times greater compared with this one in an apparatus with falling film. The maximal gain in heat transfer was from 2 to 2.5 times while the maximal gain in liquid phase mass transfer was equal to 3.5 times.

Another way of pre-swirlization of a liquid layer is the wiring in a helix in upper part of wetted tube [3], or the use of wetting device of special construction as in study of Kochetov and Bubnov [4]. Both the incision in a helix and the contraction in area permit us to obtain the enhancement of liquid phase mass transfer coefficient. The effect depends on the following parameters: the Reynolds number value, the height of a column, the spiral lead and the factor of contraction in area.

The wiring on the total active height of the apparatus was used by Saveanu *et al.* [5–7]. The studies were performed on determination of hydrodynamical characteristics of a spiral film. The enhancement of both gas and liquid phase mass transfer coefficients as well as the heat transfer intensification has been observed. The results obtained for mean thickness of a liquid film for $Re_e \in (200; 1600)$ [5] are described by the following dimensionless formula:

$$s_{r,s} = \frac{s}{\delta_e} = 4.277 + 2.7 \cdot 10^{-7} \cdot \frac{h}{\delta_e} + \left(3.849 \cdot 10^{-3} + 5.0 \cdot 10^{-4} \cdot \frac{h}{\delta_e}\right) \cdot Re_e \quad (1)$$

where

NOMENCLATURE

a_F	surface area per unit volume of packing [$m^2\ m^{-3}$]
A	exponent
C, C^*	constants
D	diameter [m]
D_A	molecular diffusivity [$m^2\ s^{-1}$]
e	roughness element width [m]
F	threaded tube surface [m^2]
F_0	smooth or equivalent to smooth tube surface [m^2]
g	gravitational acceleration [$m\ s^{-2}$]
g_0	superficial mass velocity of the liquid [$kg\ m^{-2}\ s^{-1}$]
G_A	mass exchanged [$kg\ s^{-1}$]
h	roughness height [m]
H	apparatus height [m]
k_L	average mass transfer coefficient [$m\ s^{-1}$]
l	distance between surface elements [m]
n^*	rotational speed [s^{-1}]
N	number of surface elements on apparatus active height
Re_e	film Reynolds number, $4\Gamma/\eta$
s	mean film thickness [m]
s_r	reduced film thickness, defined with equation (1)
Sc	Schmidt number, $\eta/\rho D_A$
Sh_e	modified Sherwood number, $k_L \cdot \delta_e/D_A$
t	pitch of roughness elements [m]
w	average velocity [$m\ s^{-1}$]
$X_{r,s}$	criterion of swirlization effect on mass transfer.

Greek symbols

Γ	wetting rate [$kg\ m^{-1}\ s^{-1}$]
Γ_g	characteristic geometrical modulus for rough surface
δ_e	equivalent linear dimension, defined with equation (3) [m]
ϕ_A	mass transfer intensity factor
ϕ_F	surface increasing factor
ϕ_K	overall mass transfer enhancement factor
ϕ_L	liquid phase mass transfer enhancement factor
η	viscosity [$kg\ m^{-1}\ s^{-1}$]
ρ	density [$kg\ m^{-3}$]
Θ	characteristic angle of a helix.

Subscripts

A	medium A
e	modified quantity
G	gaseous phase
k	critical value
l	laminar region
L	liquid phase
0	smooth surface
r	reduced value or rough surface/falling film
s	film thickness or spiral film
t	turbulent range
*	the value designed for real surface.

$$Re_e = \frac{4\Gamma}{\eta} \tag{2}$$

and the quantity δ_e expresses the equivalent linear dimension for liquid [8]

$$\delta_e = \sqrt[3]{\frac{\eta^2}{g \cdot \rho^2}}\,[\mathrm{m}]. \tag{3}$$

The maximal value of the factor of film thickness increase, expressed by

$$\phi_s^s = \frac{s_{r,s}}{s_{r,0}} \tag{4}$$

amount to $\phi^s_{s,max} = 2.1$ at $h = 0.5$ mm and $Re_e = 1600$. At the same time the factor of film area increase was equal to 1.102. The studies of gas phase mass transfer at $Re_e = 482$ showed that the enhancement effect will increase with a decrease of the surface elements distance and an increase of both the gas velocity and wire diameter. The maximal increase of friction factor was 14.3% at the gas phase mass transfer increase of 1.78 times. The studies of liquid phase mass transfer in spiral film [5] suggested the extreme character of the function of enhancement factor

$$\phi_L^s = \frac{Sh_{e,s}}{Sh_{e,0}} \tag{5}$$

on Reynolds number. The maximal values for mass transfer in liquid phase, dependent on wire diameter, at $Re_e = 1450$ have been observed. In this place one ought to emphasize that from two various papers of Saveanu *et al.* [5, 7] the different values of mass transfer enhancement factor ϕ_L^s result for a given diameter of metallic wire for Reynolds number values of $Re_e < 1100$ [9].

The spiral motion of thin liquid layer was obtained in the studies of desorption performed by Roj and Aksel'rod [10], but the nature of this motion was different. The water flowed down the spiral with diameter of 0.0397 m from the wire with diameter of 0.0023 m. The location of a spiral in the column axis affected the shape of a film in the form of so-called "liquid

tube". As resulted from visual observations, for small values of wetting rate the liquid flowed between the spiral elements. In the case of greater wetting a synchronous vertical flow down the film surface coexisted. The mass transfer coefficients, calculated for the doubled surface of "liquid tube", in authors' opinion [10], were comparable with results obtained by Davies and Warner [12] on the plate roughened with large-scale elements in the form of sharp-edged ridges of height running across it. The juxtaposition of the results of Roj and Aksel'rod [10] performed for $Re_e \in (60;320)$ with these obtained for $Re_e \in (680;6000)$ in [13], in my opinion, is a rather approximate conclusion.

From the above analysis it follows that in all previously known studies the additional liquid layer turbulization, the change of mean film thickness and the intensification of transfer processes, as a result of the presence of centripetal forces in spiral liquid films, have been observed. The present study is concerned with the experimental comparison of the liquid phase mass transfer coefficient enhancement for three types of surface configuration which caused the additional flow of a film along the helix.

EXPERIMENTAL

Experimental studies were carried out in equipment depicted schematically in Fig. 1. The main element of the test installation was an absorber constructed from organic glass pipe with an inside diameter of 0.140 m and a height of 1.7 m. In its axis the experimental outside wetted tubes were placed centrally. The outside diameter of a wetted tube was $D \in (0.0264;0.0392)$ [m]. The ratio of the inside diameter of a column to the outside diameter of the studied tubes with liquid film varied from 3.57 to 5.30 which warrants that the column wall effect will not take place. The height of the studied tubes was fitted by a suitable fastening of the stabilizer cap of the wetting device. The real value of effective length was determined from local values of carbon dioxide concentration when the change of those was negligible for greater values of H. The maximal values of this length attained to about 1.5 m. In Fig. 2 a schematic diagram of threaded tubes and in Table 1 a detailed characterization of the geometry of the studied pipes, have been presented. The overflow receiver prevented the pressure fluctuations in the water supply system and provided the stable temperature for a given measurement. The gas inlet pipe was equipped with the ring of the diameter of 0.120 m, on the perimeter of which the 36 inlet holes of diameter of 0.001 m have been machine-made. The measured quantities were: the water flow rate by calibrated rotameters with the scales of $[(0.83-5.00)\pm 0.08]\cdot 10^{-5}$ [$m^3\ s^{-1}$] and $[(5.0-20.0)\pm 0.2]\cdot 10^{-5}$ [$m^3\ s^{-1}$]; the inlet and outlet temperatures of the both phases with measurement accuracy of ± 0.05 K; the overpressure of carbon dioxide in apparatus; the ambient pressure and the concentration of CO_2 both in the inlet water and in the solution after absorption. The overpressure of a gas in apparatus was $\Delta P = 196$–392 [Pa]. The carbon dioxide content in inlet water was determined using the titration method with the sodium hydroxide

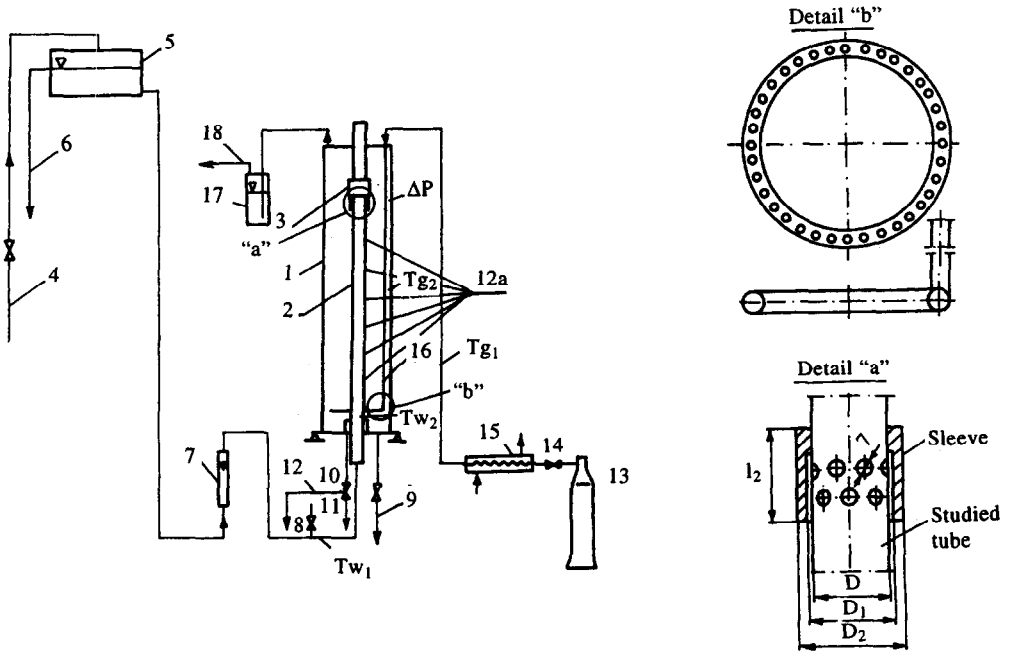

Fig. 1. Schematic diagram of experimental equipment: (1) absorber; (2) studied tube; (3) liquid distributor; (4) water inlet; (5) overflow tank; (6) water outlet; (7) rotameter; (8) deaeration valve; (9) liquid discharge after absorption; (10) three-way valve; (11) liquid spout; (12) reception of samples for analysis; (13) CO_2 gas cylinder; (14) pressure reducing valve; (15) heat exchanger; (16) gas inlet; (17) water seal; (18) gas outlet.

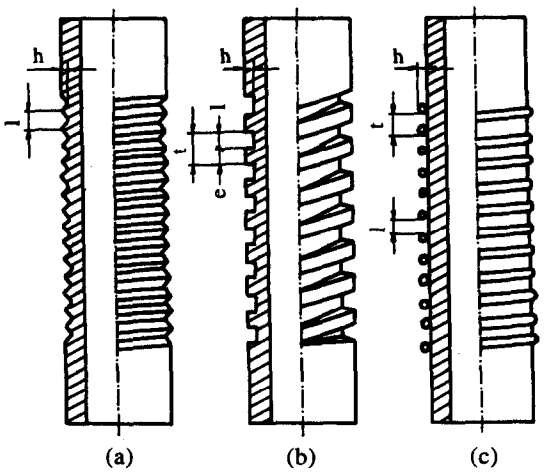

Fig. 2. Studied tubes; (a) triangular threading; (b) ribbon ribbing; (c) helical wiring.

solution of 0.05 [kmol m^{-3}] in the presence of 30% solution of Seignette's salt. The content of CO_2 in the solution after absorption was measured by potentiometric titration using of NaOH solution of the concentration of 0.1 [kmol m^{-3}]. The concentration of the absorbed gas on interface was calculated from the Henry's law constant for the average liquid temperature in a column. The measurements were carried out in the range of the mean process temperature from 281.5 to 286 K and of wetting rate $\Gamma \in (0.075; 1.094)$ [kg $m^{-1} \cdot s^{-1}$]. Γ was calculated from the following formula:

$$\Gamma = \frac{G}{\pi \cdot D}. \tag{6}$$

The studies were performed for following process and geometrical parameters: $Re_e \in (240; 3307)$, $Sc \in (833; 1126)$, $\delta_e/H \cdot 10^5 \in (3.57; 5.81)$, $h/H \cdot 10^4 \in (2.67; 11.00)$, $l/h \in (1.00; 8.00)$ and $tg\theta \in (0.0142; 0.1170)$. The tangent of characteristic angle of a helix was determined from the formula:

$$tg\theta = \frac{t}{\pi \cdot (D - 2h)}. \tag{7}$$

First the experimental data were treated mathematically, being reduced to dimensionless relationship:

$$Sh_{e,s} = C \cdot Re_e^A \cdot Sc^{0.5} \tag{8}$$

with the general assumption that the mass-transfer surface is equal to the external surface of undeformed pipes. Next the values of modified Sherwood number were calculated from the relation

$$Sh_{e,s}^* = C^* \cdot Re_s^A \cdot Sc^{0.5} \tag{9}$$

taking into account the real surface of threaded tube. The correlation values of coefficients C and C^* as well as of the exponents A of equations (8) and (9) are listed in Table 2. It must be emphasized that in the majority of previous works, instead of unknown surface of gas–liquid interface, the surface of smooth tube has been used. Only in studies of Davies *et al.* [12–16] is the real surface increase of rough tubes taken into account. The effect of surface growth was presented in the form of following ratio:

$$\phi_F = \frac{F}{F_0} \tag{10}$$

where for triangular threaded tubes (Fig. 2(a))

Table 1. Characteristics of the studied tubes

Tube no.	Material	$D/H \cdot 10^2$	N	$h \cdot 10^3$ [m]	$h/H \cdot 10^4$	l/h	t/h	$tg\theta \cdot 10^2$	ϕ_F
1	steel	2.250	515	1.50	10.01	1.939	1.939	3.0162	1.5953
2	copper	2.520	775	0.90	6.00	2.150	2.150	1.7109	1.6122
3	copper	2.513	704	1.10	7.33	1.937	1.937	1.9108	1.6489
4	copper	2.538	507	1.50	10.02	1.969	1.969	2.6856	1.6047
5	brass	2.013	1160	0.60	4.00	2.155	2.155	1.4192	1.6247
6	brass	2.013	875	0.80	5.33	2.143	2.143	1.9076	1.6050
7	brass	2.013	727	1.00	6.67	2.063	2.063	2.3286	1.6014
8	brass	2.025	570	1.30	8.67	2.012	2.012	3.0170	1.5801
9	brass	2.013	460	1.60	10.67	2.038	2.038	3.8445	1.5403
10	aluminium	2.527	500	1.50	10.00	2.000	2.000	2.7362	1.5955
				Ribbon ribbing					
11	steel	2.313	235	0.40	2.67	8.000	15.925	5.9810	1.1126
12	steel	2.512	205	1.05	7.00	6.982	6.971	6.5630	1.2531
13	steel	2.213	150	1.65	11.00	4.212	6.061	10.6460	1.2512
14	brass	1.602	276	0.60	4.01	5.217	9.050	7.5810	1.1883
15	brass	1.609	227	0.85	5.67	4.706	7.765	9.3790	1.2104
16	brass	1.599	189	1.20	8.00	4.200	6.617	11.7010	1.2303
				Helical wiring					
17	copper	2.003	832	0.90	6.01	1.000	2.000	2.0318	1.6130
18	copper	1.981	555	0.90	6.00	2.000	3.000	3.0804	1.3885
19	copper	2.009	416	0.90	6.01	3.000	4.000	4.0492	1.2776

Table 2. Correlation constants and exponents in equations (8) and (9)

Material	Tube no.	Range of validity	A	$C\cdot10^3$	$C^*\cdot10^3$	Range of validity	A	$C\cdot10^3$	$C^*\cdot10^3$
Steel	1	$Re_e\in(317;822)$	0.510	8.119	5.089	$Re_e\in(822;2810)$	1.003	0.2968	0.1860
Copper	2	$Re_e\in(255;900)$	0.425	10.93	6.779	$Re_e\in(900;2473)$	1.056	0.1495	0.0927
Copper	3	$Re_e\in(262;884)$	0.448	10.83	6.570	$Re_e\in(884;2612)$	1.072	0.1571	0.0953
Copper	4	$Re_e\in(240;816)$	0.465	11.52	7.176	$Re_e\in(816;2729)$	1.095	0.1686	0.1050
Brass	5	$Re_e\in(261;938)$	0.426	7.349	4.523	$Re_e\in(938;2740)$	0.927	0.2384	0.1468
Brass	6	$Re_e\in(280;914)$	0.452	7.495	4.670	$Re_e\in(914;2847)$	0.948	0.2548	0.1588
Brass	7	$Re_e\in(323;879)$	0.468	7.654	4.779	$Re_e\in(879;2400)$	0.967	0.2599	0.1623
Brass	8	$Re_e\in(335;832)$	0.494	7.918	5.010	$Re_e\in(832;2538)$	0.991	0.2800	0.1773
Brass	9	$Re_e\in(312;794)$	0.508	8.195	5.321	$Re_e\in(794;2674)$	1.011	0.2851	0.1851
Aluminium	10	$Re_e\in(308;845)$	0.494	9.328	5.846	$Re_e\in(845;2490)$	1.036	0.2551	0.1600
Steel	11	$Re_e\in(280;676)$	0.648	3.011	2.705	$Re_e\in(676;2570)$	1.036	0.2403	0.2159
Steel	12	$Re_e\in(284;764)$	0.634	3.259	2.600	$Re_e\in(764;2600)$	1.028	0.2383	0.1901
Steel	13	$Re_e\in(296;923)$	0.589	3.975	3.176	$Re_e\in(923;3209)$	1.007	0.2290	0.1830
Brass	14	$Re_e\in(290;870)$	0.600	3.630	3.054	$Re_e\in(870;3180)$	1.006	0.2325	0.1956
Brass	15	$Re_e\in(290;892)$	0.592	3.729	3.081	$Re_e\in(892;3214)$	1.003	0.2285	0.1888
Brass	16	$Re_e\in(284;911)$	0.581	3.825	3.109	$Re_e\in(911;3307)$	0.997	0.2248	0.1825
Copper	17	$Re_e\in(321;935)$	0.426	14.23	8.822	$Re_e\in(935;2580)$	0.769	1.362	0.8444
Copper	18	$Re_e\in(320;968)$	0.400	15.10	10.88	$Re_e\in(968;2700)$	0.746	1.399	1.008
Copper	19	$Re_e\in(350;1024)$	0.383	16.42	12.85	$Re_e\in(1024;2820)$	0.720	1.588	1.243

$$F = N\cdot l\cdot\sqrt{(4h^2+l^2)\cdot(1+ctg^2\theta)} \tag{11}$$

for ribbon ribbing (Fig. 2(b))

$$F = N\cdot[t\cdot(t+2h)\cdot\sqrt{1+ctg^2\theta}+2\pi\cdot h\cdot(e+h)] \tag{12}$$

and for helical wiring (Fig. 2(c)) properly

$$F = N\cdot\left[t\cdot\left(1+\frac{3\pi\cdot h}{4}\right)\cdot\sqrt{1+ctg^2\theta}+\frac{3}{4}\cdot\pi^2\cdot h^2\right]. \tag{13}$$

In Figs. 3–5 the experimental results of the present study have been presented. For better presentation of the enhancement of mass transfer in spiral film, the limit of theoretical probability of the process in smooth-wall apparatus [11] has been additionally distinguished (designed with axis-lines /-.-.-./). The values of $Sh_{e,s}$ for all studied tubes except two (tube no. 5 for $Re_e \leqslant 1050$ and tube no. 6 for $Re_e < 505$) are greater than the maximal values of $Sh_{e,0}$ characteristic for a falling film. The best result taking into account the values of $Sh_{e,s}$ has been observed for the tubes with triangular threading no. 1 and 10 ($\Gamma_g \cong 10$). The modified Sherwood number values $Sh^*_{e,s}$ lie particularly in the region of the theoretical

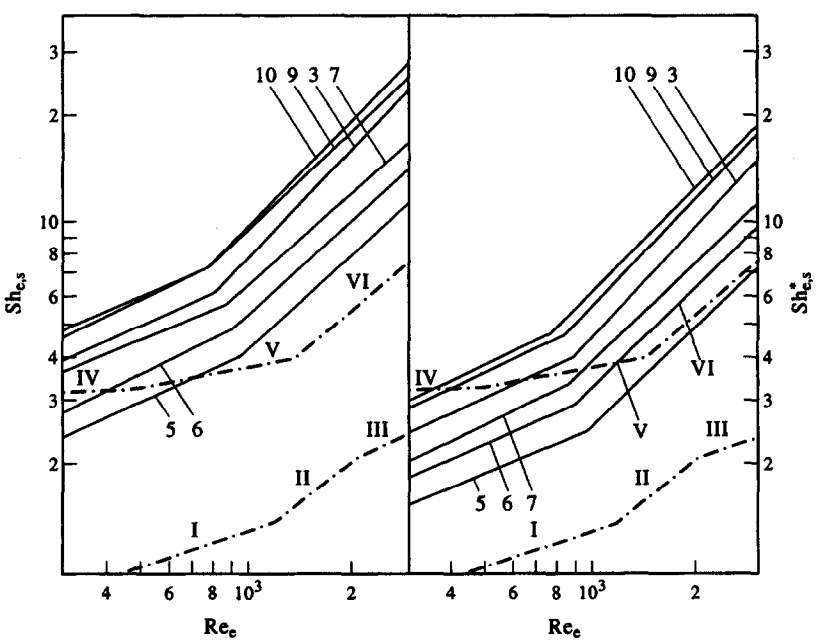

Fig. 3. Experimental results for chosen triangular threaded tube presented for $T = 284$ K (designation of the lines corresponds with the tube numeration given in Table 1). ····· theoretical relations for smooth-wall film-apparatus: (I) Pigford [17, 18] and Brötz [19, 20]; (II) Brötz [19, 20]; (III) Stirba and Hurt [21]; (IV) Yih and Chen [22, 23]; (V, VI) Kulov *et al.* [24].

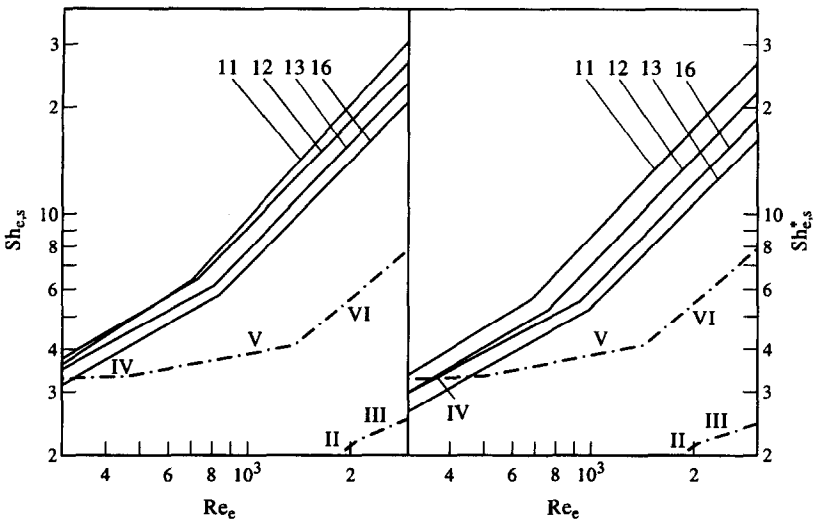

Fig. 4. Experimental results for chosen ribbon ribbed tubes presented for $T = 284$ K (designation of the lines corresponds with the tube numeration given in Table 1). ····· theoretical relations for smooth-wall film-apparatus as in Fig. 3.

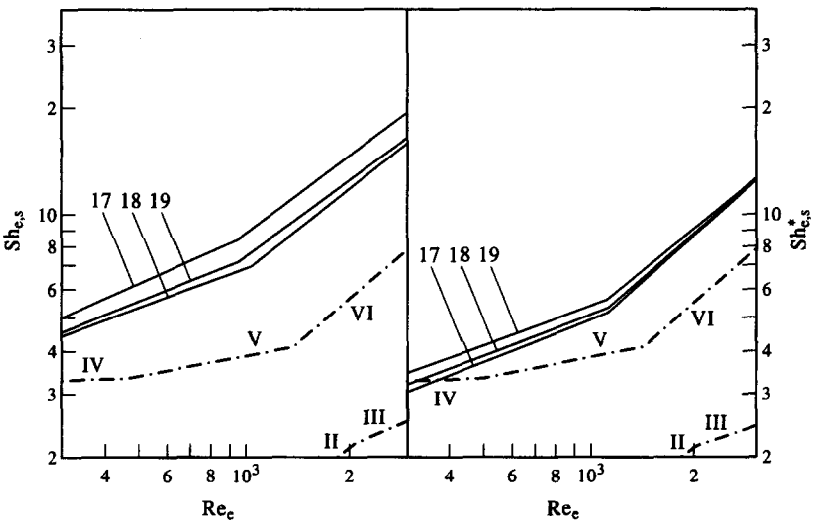

Fig. 5. Experimental results for helical wired tubes presented for $T = 284$ K (designation of the lines 17–19 corresponds with the tube numeration given in Table 1). ····· theoretical relations for smooth-wall film-apparatus as in Fig. 3.

probability of mass transfer in a film flowing down smooth surface [11] and particularly on the upper side of the limit of this region. The maximal values of $Sh^*_{e,s}$ have been obtained for ribbon ribbed steel tube with characteristics: $\Gamma_g = 8$ and $tg\theta = 0.05980$. An analysis of the experimental data showed that the spiral motion of a liquid thin layer causes the decrease (in comparison with falling film) of the Reynolds number value characteristic for the beginning of turbulent process mechanism. This effect is described by the following general formula:

$$\Delta Re^s_{e,c,t} = Re^0_{e,c,t} - Re^s_{e,c,t} a \cdot \Gamma_g + b \qquad (14)$$

where $Re^s_{e,c,t}$ is the critical value of Reynolds number for spiral film; $Re^0_{e,c,t}$ is the critical value of Reynolds number for film flowing down smooth surface (for steel $Re^0_{e,c,t} = 1060$; for copper $Re^0_{e,c,t} = 1050$; for brass $Re^0_{e,c,t} = 1030$; for aluminium $Re^0_{e,c,t} = 970$ from [12]); Γ_g is the factor of the surface characteristics (for triangular threading $\Gamma_g = h/H \cdot 10^4$; for ribbon and wiring: $\Gamma_g = l/h$).

DISCUSSION

In order to compare the presented data with the results of other studies, the heights of mass transfer unit have been determined too. In Fig. 6 the values of $H_L = f(Re_e)$ for three tubes of various surface configuration with the maximal effect of mass transfer coefficient increase have been compared with the representative data for packed columns [26–28] and "liquid tube" [10]. The equivalent Reynolds number

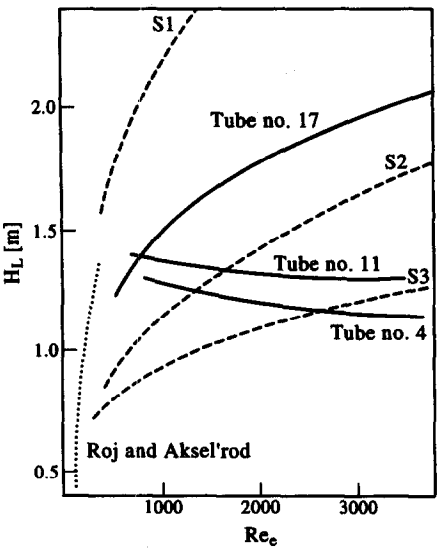

Fig. 6. Comparison of the H_L values for chosen studied tubes with the representative values for the packed columns (- - -) and for the "liquid tube" [10] (· · ·). (S1) Van Krevelen and Hoftijzer [26]; (S2) Fujita and Hayakawa [27]; (S3) Sherwood and Holloway [28].

for packing was calculated from the following formula:

$$Re_e = \frac{4g_0}{a_F \cdot \eta} \tag{15}$$

where g_0 is the superficial mass velocity of the liquid, referred to the cross-section of the "empty" tower and a_F—the surface area per unit volume of packing. Obtained values of liquid phase mass transfer unit heights for spiral films are comparable with the data known for packed columns.

In [11, 25] it has been stated that in a liquid film flowing gravitationally down smooth and rough tubes the wall effect on transfer processes is evident. The significant discrepancies between different data known from literature called for inquiries about the estimation criteria of real enhancement of mass transfer in spiral films. Two types of the criteria have been analysed: the first, based on the values of quantities calculated for the surface of smooth tubes ($Sh_{e,s}$) and the second, with respect to wall surface increase factor ($Sh^*_{e,s}$). The values for equivalent smooth tubes formed the first datum level. The criteria taken as the mass transfer enhancement factors were defined as follows:

$$\phi^s_L = \frac{Sh_{e,s}}{Sh_{e,0}}; \quad \phi^{s,*}_L = \frac{Sh^*_{e,s}}{Sh_{e,0}}. \tag{16}$$

The values of $Sh_{e,o}$ calculated from the formula

$$Sh_{e,0} = C_0 \cdot Re_e^{A_0} \cdot Sc^{0.5} \tag{17}$$

with correlation values of C_0 and A_0 for studied materials are listed in Table 3. The second datum level was found on the basis of the values of $Sh_{e,r}$ and $Sh^*_{e,r}$ in a film flowing gravitationally down triangular and ring grooved tubes [25]. The criteria on the film swirlization effect are introduced as the following ratios:

$$X_{r,s} = \frac{Sh_{e,s}}{Sh_{e,r}} = \frac{\phi^s_L}{\phi^r_L}; \quad X^*_{r,s} = \frac{Sh^*_{e,s}}{Sh^*_{e,r}} = \frac{\phi^{s,*}_L}{\phi^{r,*}_L}. \tag{18}$$

In Figs. 7 and 8 the relations of $\phi^s_L = f(Re_e)$, $\phi^{s,*}_L = f(Re_e)$ and the effect of parameters of surface characteristics for a given Re_e, have been presented. For triangular threading the mass transfer enhancement factor increases with increasing of surface wetting rate as well as of the values of both Γ_g and the characteristic angle of a helix. For ribbon ribbed flow surfaces the increasing of the enhancement factors with increase of both the Reynolds number values and

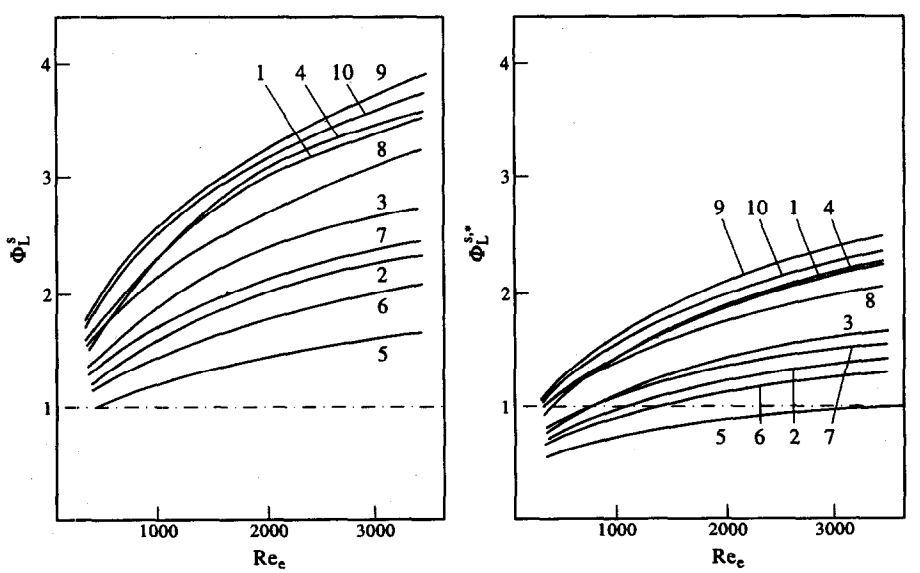

Fig. 7. Reynolds number effect on the process enhancement factors ϕ^s_L and $\phi^{s,*}_L$ for the tubes with triangular threading (designation of the lines corresponds with the one given in Table 1).

Table 3. Values of constants and exponents in equation (17) from [11]

Material	Range of validity	A_0	$C_0 \cdot 10^2$	Range of validity	A_0	$C_0 \cdot 10^2$	Range of validity	A_0	$C_0 \cdot 10^4$
Steel	$Re_e \leqslant 370$	0.383	1.029	$Re_e \in (370; 1060)$	0.250	2.259	$Re_e \in (1060; 2643)$	0.714	8.923
Copper	$Re_e \leqslant 320$	0.309	1.795	$Re_e \in (320; 1050)$	0.213	3.122	$Re_e \in (1050; 2708)$	0.802	5.187
Brass	—	—	—	$Re_e \in (300; 1030)$	0.244	2.188	$Re_e \in (1030; 2810)$	0.707	8.817
Aluminium	—	—	—	$Re_e \in (308; 970)$	0.230	2.552	$Re_e \in (970; 2490)$	0.738	7.750

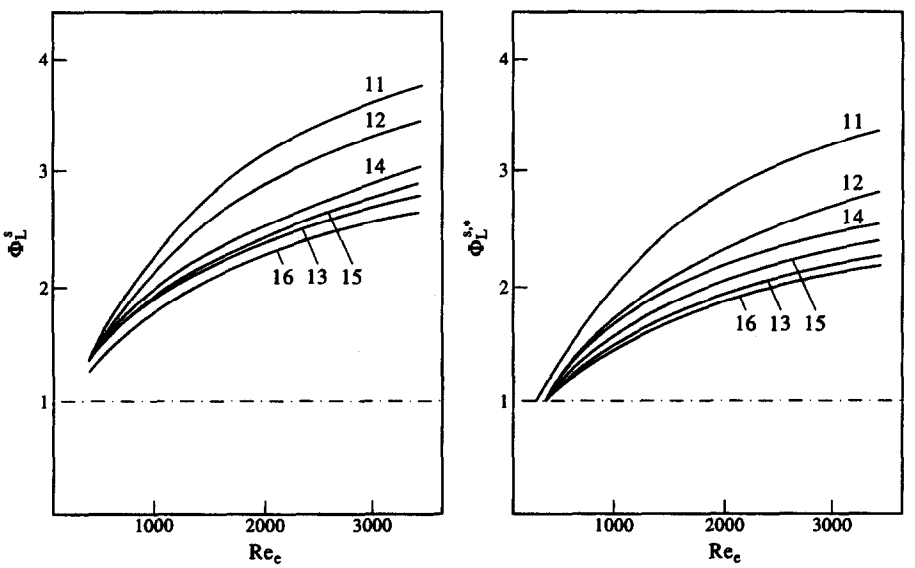

Fig. 8. Reynolds number effect on the process enhancement factors ϕ_L^s and $\phi_L^{s,*}$ for the tubes with ribbon ribbing (designation of the lines corresponds with this one given in Table 1).

Table 4. The correlation values of the coefficients in equation (19)

Surface type	Range of Re_e	C_1	A_1	C_2	A_2	C_3	A_3
Triangular threading	$Re_e < Re^s_{e,c,t}$	0.520	0.102	0.110	0.375	0.386	0.148
	$Re_e > Re^s_{e,c,t}$	0.652	0.202	0.142	0.316	0.483	0.247
Ribbon ribbing	$Re_e < Re^s_{e,c,t}$	0.422	0.391	0.235	0.253	0.276	0.295
	$Re_e > Re^s_{e,c,t}$	0.214	−0.082	0.233	0.153	0.139	−0.178
Helical wiring	$Re_e < Re^s_{e,c,t}$	0.995	0.202	0.214	−0.203	2.323	0.542
	$Re_e > Re^s_{e,c,t}$	5.842	0.210	−0.0328	0.801	13.65	0.550

the geometrical modulus Γ_g and decrease of the angle θ, has been observed. The functions of $\phi_L^s = f(Re_e)$ and $\phi_L^{s,*} = f(Re_e)$ for helical wired tubes were of an extreme character with maximum for $Re_e = Re^0_{e,c,t} = 1050$. As a result of the elaboration of experimental data the general formulas for the enhancement factors:

$$\phi_L^s = C_1 \cdot (tg\theta)^{A_1} \cdot Re_e^{C_2 \cdot \Gamma^{A_4}};$$

$$\phi_L^{s,*} = C_3 \cdot (tg\theta)^{A_3} \cdot Re_e^{C_2 \cdot \Gamma^{A_4}} \qquad (19)$$

have been obtained. In Table 4 the correlation values of the characteristic coefficients of equation (19) have been presented.

In Figs. 9 and 10 (with the legend listed in Table 5) the enhancement of mass transfer obtained in present study was compared with the studies performed for film pre-swirlization [1, 29]. The factor ϕ_A^s in the study of Carre and Bugarel [1] was defined as follows:

$$\phi_A^s = \frac{G_{A,s}}{G_{A,0}}. \qquad (20)$$

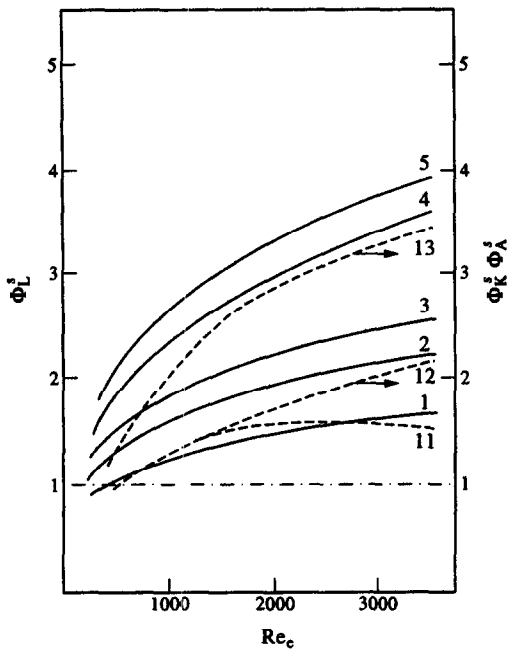

Fig. 9. Comparison of the process intensification factor ϕ_L^s values for triangular threading with results from various papers. The legend of the lines is given in Table 5.

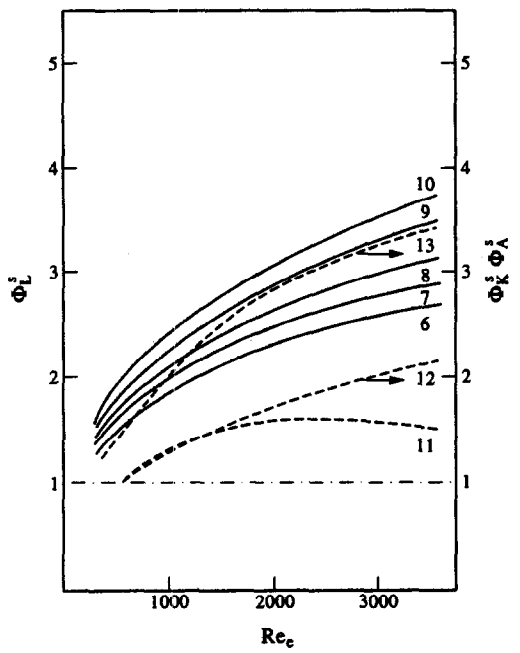

Fig. 10. Comparison of the process intensification factor ϕ_L^s values for ribbon ribbing with results from various papers. The legend of the lines is given in Table 5.

From the patterns showed in Figs. 9 and 10 it follows that the enhancement of the process for passive turbulization of liquid film depends on Reynolds number. The values of ϕ_L^{s*} for some studied tubes are comparable with the data of Carre and Bugarel [1]. In this place one ought to emphasize that the values of ϕ_A^s are on the average about 57% greater than the values of ϕ_k^s.

The analysis of the criteria of film swirlization effect was made for two types of wall shape: triangular threading and ribbon ribbing. Accordingly the quantities of ϕ_L^s and ϕ_L^{s*}, have been calculated from the adequate general relations for triangular and ring grooved surfaces [25]. The values of $X_{r,s}$ (Figs. 11 and 12) for all tubes studied (except tube no. 5 for $Re_e < 840$) were $X_{r,s} > 1$. For ribbon ribbed tubes

$$X_{r,s}^* \cong X_{r,s} = 0.6814 \cdot Re_e^{0.0487 \cdot \Gamma_g^{0.337}} > 1. \quad (21)$$

The values of $X_{r,s}^* > 1$ were obtained for the triangular threaded tubes for $tg\theta = 0.02$ in total studied range of surface wetting rate. For the characteristic angles of a helix $\theta \in (0.01419\pi; 0.01911\pi)$ this effect is limited from below by the correlation:

$$Re_{e,c,X} = 1.826 \cdot 10^{-9} \cdot (tg\theta)^{-6.645}. \quad (22)$$

As a result of mathematical elaboration of the present data for mass transfer into a liquid film flowing down tubes with triangular threaded surfaces the general relations have been obtained. These are as follows; for transitional range of a process

$$X_{r,s} = 0.928 \cdot (tg\theta)^{0.102} \cdot Re_e^{0.0412 \cdot \Gamma_g^{0.487}};$$

$$X_{r,s}^* = 0.921 \cdot (tg\theta)^{0.148} \cdot Re_e^{0.0412 \cdot \Gamma_g^{0.487}} \quad (23)$$

for turbulent range of a process

$$X_{r,s} = 0.0567 \cdot (tg\theta)^{-0.412} \cdot Re_e^{0.0676 \cdot \Gamma_g^{0.613}};$$

$$X_{r,s}^* = 0.0712 \cdot (tg\theta)^{-0.412} \cdot Re_e^{0.0676 \cdot \Gamma_g^{0.613}}. \quad (24)$$

The maximal values of the criteria of film swirlization effect have been obtained for the triangular threaded tubes no. 10 ($X_{r,s(Re_e=3000)} = 2.37$; $X_{r,s(Re_e=3000)}^* = 2.02$) and no. 9 ($X_{r,s(Re_e=3000)} = 2.26$; $X_{r,s(Re_e=3000)}^* = 2.00$). Accordingly for the best of the ribbon ribbed tubes (no. 11) for $Re_e = 3000$ these values were $X_{r,s}^* \cong X_{r,s} = 1.50$. These numerical examples show that the effect of the spiral motion of a film is stronger in the case of triangular incisions than in the case of ribbon ribbing.

It is not possible to compare the obtained values of the criteria of film swirlization effect with other existing data. Most of the previously published studies have been confined to one type of regular wall roughness. As an exception, the paper of Moalem-Maron, Sideman and Horn [30] may be pointed out. These experimental studies have been performed on liquid phase mass transfer on horizontal tubes of both elliptic and circular cross-sections, smooth as well as ring grooved and ribbon ribbed. In common ranges of Reynolds number $Re_e \in (300; 600)$ the analogy of the effect of characteristic angle of a helix on $X_{r,s}$ values has been observed. The increase of the angle θ causes the decrease in the value of the criterion of film swirlization effect.

Table 5. Legend for Figs. 9 and 10

No.	Results	Process enhance type	Quantity	Γ_g	$tg\theta$
1	own	triangular threading	ϕ_L^s ; ϕ_L^{s*}	4.0	0.01419
2	own	triangular threading	ϕ_L^s ; ϕ_L^{s*}	6.0	0.01711
3	own	triangular threading	ϕ_L^s ; ϕ_L^{s*}	7.3	0.01911
4	own	triangular threading	ϕ_L^s ; ϕ_L^{s*}	10.0	0.02686
5	own	triangular threading	ϕ_L^s ; ϕ_L^{s*}	10.67	0.03845
6	own	ribbon ribbing	ϕ_L^s ; ϕ_L^{s*}	4.2	0.11701
7	own	ribbon ribbing	ϕ_L^s ; ϕ_L^{s*}	4.7	0.09379
8	own	ribbon ribbing	ϕ_L^s ; ϕ_L^{s*}	5.2	0..07581
9	own	ribbon ribbing	ϕ_L^s ; ϕ_L^{s*}	7.0	0.06563
10	own	ribbon ribbing	ϕ_L^s ; ϕ_L^{s*}	8.0	0.05981
11	Sergeev [29]	preswirlization	ϕ_L^s ; ϕ_L^{s*}	—	—
12	Carre and Bugarel [1]	preswirlization	ϕ_k^s	—	—
13	Carre and Bugarel [1]	preswirlization	ϕ_A^s	—	—

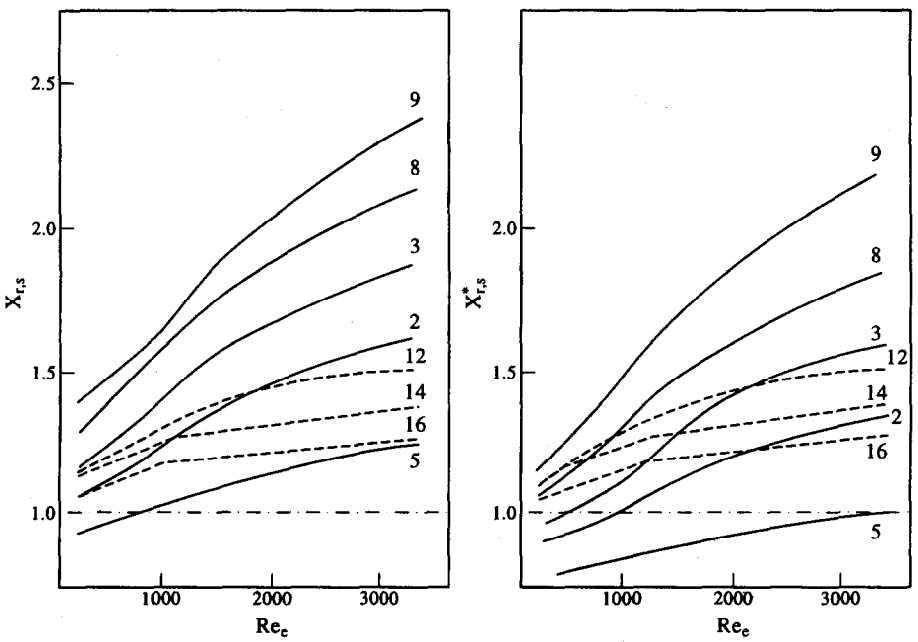

Fig. 11. Dependence of the criterion of liquid film swirling effect on Reynolds number (designation of the lines corresponds with the tube numbering given in Table 1): — triangular threading; - - - ribbon ribbing.

CONCLUSION

The experimental studies of mass transfer process intensification in a liquid film for three types of the outside tube surface configuration, forced by the additional flow along the helix, have been presented. The positive effect of the ribbing in a helix in comparison with the incisions perpendicular to apparatus axis of the similar form, has been found. The process intensification factors as the functions of Reynolds number and characteristic for a given surface configuration geometrical parameter as well as of characteristic angle of a helix have been presented. It has been shown that the maximal value of process enhancement factor with respect to smooth surfaces from the given material was 3.75 (with regard to surface expansion factor of 3.19) and the liquid film swirlization can improve the process kinetics even by 2.4 times (with regard to wall surface expansion about twice) in comparison with the effect obtained for a respective ribbed surface, while not forcing the spiral motion of a layer.

Acknowledgements—The author is indebted to the Ministry of National Education of Poland, under the auspices of

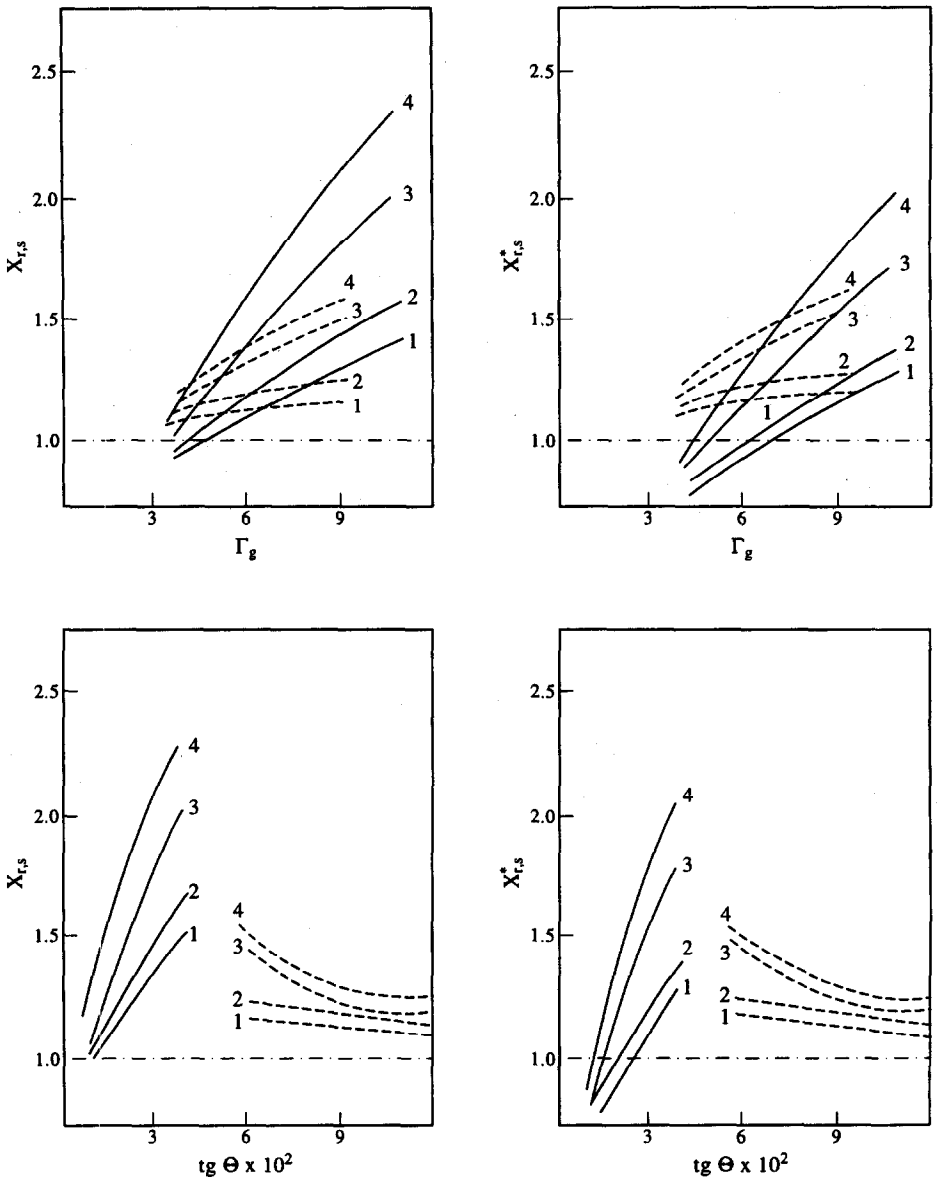

Fig. 12. Surface geometrical parameters effect on the value of criterion of the liquid film swirling effect: — triangular threading; - - - ribbon ribbing; (1) $Re_c = 400$; (2) $Re_c = 700$; (3) $Re_c = 1500$; (4) $Re_c = 2500$.

whom this work was carried out. The work was also supported by KBN donation for Institute activity DS no. 32/226.

REFERENCES

1. Carre, B. and Bugarel, R., Determination experimental de l'accroissement de la surface offerta a l'echange de mass par un "film spirale" par rapport a "un cylindrical tombant". *Chemical Engineering Science*, 1969, **24**, 921–936.
2. Larranaga, F. J., Mora, J. C. and Bugarel, R., Wetted wall columns with tangential liquid feed: advantages for heat and mass transfer, multitubular exchanger. Scientifique Reports de Institut du Genie Chimique de Toulouse, private communication, Toulouse, 1985.
3. Brauer, H., Strömung and Wärmeübergang bei Rieselfilmen. *VDI-Forschungsheft*, 1956, **457**, 1–40.
4. Kochetov, N. M. and Bubnov, Yu. I., Carbon dioxide absorption in film column. *Izvestiya vuzoz, Khimiya i khimicheskaya tekhnologiya*, 1975, **18**, 474–476.
5. Saveanu, T., Ibanescu, I. and Vasiliu, M., Analysis of intensification of transfer processes in countercurrent gas–liquid film flow by means of roughness. *Bulletin de l'Institut politechnica Iasi, Serie Noua*, 1962, **3–4**, 129–140.
6. Saveanu, T., Ibanescu, I. and Vasiliu, M., Effect of the surface roughness on mass transfer in liquid wavy film flow. *Studii si Cercetari Stiintica Chimie*, 1960, **21**, 149–157.
7. Saveanu, T., Ibanescu, I. and Vasiliu, M., Critical value of Reynolds number in film flow. *Revue Chimica (Bucharest)*, 1962, **13**, 589–592.
8. Hobler, T., *Mass Transfer and Absorbers*. Pergamon Press, London, 1966, p. 128
9. Broniarz, L., Enhancement of the transfer processes using the passive turbulization of a film, *Wydawnictwo*

Politechniki Poznańskiej/Poznań University of Technology Publ./, Seria Rozprawy, 1991, **253,** Poznań.
10. Roj, D. K. and Aksel'rod, L. S., Study on hydrodynamics and mass transfer in spiral-film column with single element. *Teoreticheskie osnovy khimicheskoj tekhnologii*, 1974, **8,** 17–21.
11. Broniarz, L., Wall of film apparatus effect on mean thickness of liquid film and liquid phase mass transfer coefficient. *Inżynieria Chemiczna i Procesowa*, 1991, **12,** 227–249.
12. Davies, J. T. and Warner, K. V., The effect of large-scale roughness in promoting gas absorption. *Chemical Engineering Science*, 1969, **24,** 231–240.
13. Davies, J. T., *Turbulence Phenomena.* Academic Press, New York, 1972.
14. Davies, J. T. and Shawki, A. M., Enhancement of turbulent heat transfer. *Chemical Engineering*, 1973, **279,** 528–532.
15. Davies, J. T. and Shawki, A. M., Heat transfer from turbulent falling films of water and non-Newtonian solutions on smooth and ridged plates. *Chemical Engineering Science*, 1974, **29,** 1801–1808.
16. Davies, J. T. and Lozano, F. J., Turbulence characteristics and mass transfer at air–water surfaces, *American Institute of Chemical Engineers Journal*, 1979, **25,** 405–415.
17. Emmert, R. E. and Pigford, R. L., *Absorption and Extraction.* McGraw Hill, New York, 1952.
18. Sherwood, T. K. and Pigford, R. L., *Absorption and Extraction.* McGraw Hill, New York, 1952.
19. Brötz, W., Über die Vorausberechnung der Absorptionsgeschwindigkeit von Gasen in strömenden Flüssigkeitesschichten. *Chemie-Ingenieur-Technik*, 1954, **26,** 470–478.
20. Brötz, W., *Grundriss der Chemischen Reaktionstechnik.* Verlag Chemie, Weinheim, 1975.
21. Stirba, C. and Hurt, D. M., Turbulence in falling liquid films. *American Institute of Chemical Engineers Journal*, 1955, **1,** 178–184.
22. Yih, S. M. and Chen, K. Y. *Chemical Engineering Communication*, 1982, **17,** 123, from [23].
23. Yih, S. M., Modeling of heat and mass transport in falling liquid films. *Handbook of Heat and Mass Transfer*, Vol. 2. Mass transfer and reactor design, Gulf, Houston, Tx, 1986, pp. 111–210.
24. Kulov, N. N. *et al.*, Mass transfer in falling liquid films. *Teoreticheskie osnovy khimicheskoj tekhnologii*, 1983, **17,** 291–306.
25. Broniarz, L., Enhancement of transfer processes in gravity liquid film flow. II. Effect of triangular and ring grooving on liquid phase mass transfer. *Inżynieria Chemiczna i Procesowa*, 1992, **13,** 285–307.
26. Van Krevelen, D. W., Hoftijzer, P. J. and Van Hooren, C. J., Gasabsorptionsstudien, Teil I–IV. *Recueil de Travaux Chimiques des Pays-Bas*, 1947–1950.
27. Fujita, S. and Hayakawa, T., *Kagaku kogaku*, 1956, **20,** 113–117, from Ramm, V. M., *Gas Absorption.* Khimiya, Moscow, 1976.
28. Sherwood, T. K. and Holloway, P. A. L., *Transactions of the American Institute of Chemical Engineers*, 1940, **36,** 21–70, from [18].
29. Sergeev, G. I., On the mass transfer enhancement in film flow. *Sbornik trudov Vsesojuznogo ob'edinija "Neftekhim"*, 1976, **11,** 122–130.
30. Moalem-Maron, D., Sideman, S. and Horn, H., Enhanced film mass transfer coefficients on grooved horizontal conduits. *Chemical Engineering Science* 1979, **34,** 420–425.